

## Chemical treatment of mica for atomic force microscopy can affect biological sample conformation

Lilian T. Costa<sup>a,b</sup>, José R. Pinto<sup>c</sup>, Marta B. Moraes<sup>a</sup>, Guttierre G.B. de Souza<sup>a</sup>,  
Martha M. Sorenson<sup>c</sup>, Paulo M. Bisch<sup>a</sup>, Gilberto Weissmüller<sup>a,\*</sup>

<sup>a</sup>*Instituto de Biofísica Carlos Chagas Filho, Universidade Federal do Rio de Janeiro, Rio de Janeiro 21949-900, Brazil*

<sup>b</sup>*Centro de Biotecnologia, Universidade Federal do Rio Grande do Sul, Porto Alegre 91500-970, Brazil*

<sup>c</sup>*Departamento de Bioquímica Médica, Instituto de Ciências Biomédicas, Universidade Federal do Rio de Janeiro, Rio de Janeiro 21941-590, Brazil*

Received 6 May 2003; received in revised form 7 October 2003; accepted 7 October 2003

### Abstract

An important aspect in the preparation of substrate materials to use in atomic force microscopy lies in the question of interactions introduced by treatments designed to immobilize the sample over the substrate. Here we used a mica substrate that was chemically modified with cationic nickel to immobilize actin filaments (F-actin). Chemical modification could be followed quantitatively by measuring the interaction force between the scanning tip and the mica surface. This approach allowed us to observe polymeric F-actin in a structure that resembles an actin gel. It also improved sample throughput and conferred sample stability as well as repeatability from run to run.

© 2003 Elsevier B.V. All rights reserved.

**Keywords:** Actin gel; Atomic force microscopy; Ni; Mica; Surface functionalization

### 1. Introduction

Atomic force microscopy (AFM) is a useful tool for elucidating the surface topography of biomolecules, including proteins [1]. In addition, it has begun to be used for force spectroscopy measurements based on tip control, which reveals further surface properties such as elasticity and adhesiveness [2]. The forces measured with AFM range from piconewtons to nanonewtons [3]. It has

also proven to be advantageous for obtaining high resolution at a molecular level, since it yields images in air as well as under physiological conditions [4]. Nevertheless, one of the most difficult steps in preparing samples for AFM is to immobilize the molecules on a flat surface, so that they can be visualized or manipulated without detaching them.

Mica is commonly used as a substrate for AFM imaging at molecular resolution due to its atomically flat surface. However, it is notoriously difficult to immobilize negatively charged samples [5], because binding to the substrate is not strong enough to avoid moving the samples or sweeping

\*Corresponding author. Tel.: +55-21-2562-6575; fax: +55-21-2280-8193.

E-mail address: gilberto@biof.ufrj.br (G. Weissmüller).

them entirely away with the scanning tip. In order to increase its affinity for negatively charged samples, mica has been chemically treated with divalent cations, such as nickel ( $\text{Ni}^{2+}$ ) [6–8]. This treatment has been used successfully in preparing DNA for AFM imaging, resulting in greater stability and no apparent change in conformation. Other authors attached genetically engineered histidine tags to a specific molecular region in an elegant but time-consuming procedure that made it possible to immobilize IgG in a homogeneous orientation on  $\text{Ni}^{2+}$ -treated mica [9].

Actin is a highly conserved protein found in every eukaryotic cell studied so far, and is a major component of the cytoskeleton [10,11]. The functional form of actin in cells is a double-stranded, filamentous polymer containing multiple copies of the globular actin (G-actin) monomer with ADP and  $\text{Mg}^{2+}$  or  $\text{Ca}^{2+}$  bound to the hydrophobic core [12]. In the presence of specific actin-binding proteins, actin filaments (F-actin) form a 3D network [13] in which the linear polymer becomes a mechanically rigid gel because of interpolymer junctions that link the filaments in an infinite network. Actin alone can mediate motility through controlled polymerization or through gel–sol structural transitions [14]. Molecular models of the filament structure have been investigated by AFM [15,16]. However, actin filaments could be imaged on freshly cleaved mica only at pH 6 or lower, and after stabilization with phalloidin [17]. Stable images were also obtained using cryoatomic force microscopy; to prevent depolymerization, filaments were labeled with phalloidin [15]. Another means of immobilizing actin was to use lipid bilayers on the mica surface [16]. This procedure was successful for imaging actin paracrystals, but not for individual filaments.

In this work, we used mica chemically treated with  $\text{Ni}^{2+}$  (Ni-mica) to increase the affinity between mica and F-actin. However, when F-actin suspended in buffer is applied to Ni-mica, the structure resembles an actin gel. This gel is stable and does not appear to be altered by the probe scan. We are not aware of any previous AFM studies of actin gels in aqueous solution.

## 2. Materials and methods

### 2.1. F-actin purification and polymerization

G-actin was purified from chicken skeletal muscle and polymerized to F-actin from acetone powder following the method described by Pardee and Spudich [18]. F-actin was stored as a pellet at 0 °C overnight and just before use was resuspended at  $\sim 10$  mg/ml in actin buffer (20 mM imidazole-HCl, pH 7.0, 5 mM  $\text{MgCl}_2$ , 0.5 mM  $\text{K}_2\text{EGTA}$ , 2 mM  $\text{Na}_2\text{K}_2\text{ATP}$ , 6.5 mM KCl, 1.5 mM  $\text{NaN}_3$  and 1 mM dithiothreitol). Dilution to working concentrations (see Figure legends) was carried out using Millipore-filtered buffer (0.22  $\mu\text{m}$  pore size). The concentration was determined by the biuret reaction [19]. In SDS-PAGE on 12% acrylamide gels stained with Coomassie blue a single band was observed, without contamination by other proteins (not shown).

### 2.2. Mica treatment

Mica (Plano GmbH, Wetzlar, Germany) was prepared according to a modification of a protocol already described in Refs. [5,20]. Freshly cleaved mica films were immersed in 1 mM  $\text{NiCl}_2$  (Vetec Química Fina Ltda., Rio de Janeiro, Brazil) and left at room temperature overnight (12 h). The films were removed from the salt solution and ultrasonicated three times for 10 min in fresh lots of de-ionized water (Milli-Q resins from Millipore Corp., Bedford, MA) to remove excess salt. After drying under a vacuum at room temperature, the films were stored in a desiccator until used.

### 2.3. Deposition of F-actin

Each sample was deposited on treated or untreated mica film over an area of  $\sim 1$  cm<sup>2</sup>. After several trials, this procedure was standardized, so that approximately 4  $\mu\text{l}$  F-actin was applied to the film. After 5 min, the sample was analyzed with AFM.

### 2.4. Atomic force microscopy

Both images and force curves were recorded using a homemade AFM. Coverslips were glued

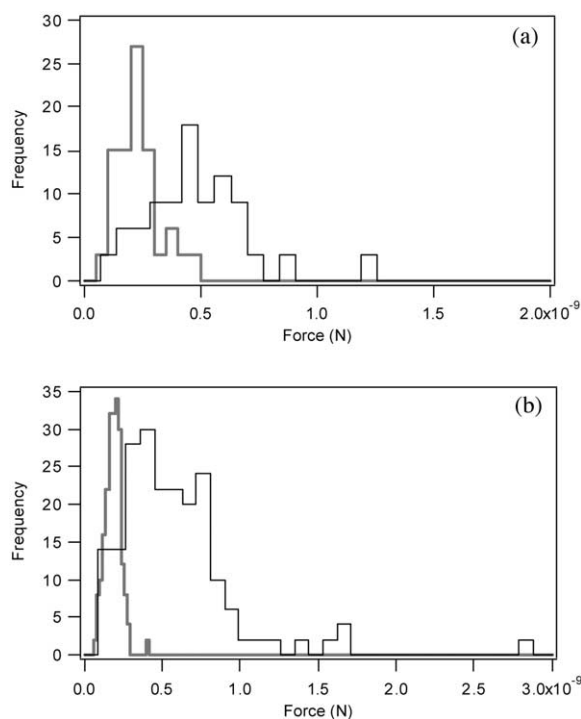


Fig. 1. Force–frequency histograms of tip–substrate interaction, comparing untreated mica (gray lines) and Ni-mica (black lines) in actin buffer (a) and in PBS (b).

to magnetic stainless-steel punches and mounted in a fluid cell, without using an O-ring. Samples were scanned in contact error mode at room temperature using a standard silicon nitride tip (Digital Instruments Inc., Santa Barbara, CA) with a  $4\text{-}\mu\text{m}^2$  pyramidal base mounted on a V-shaped cantilever of spring constant  $0.06\text{ N/m}$ . The cantilever was cleaned by placing it under a mercury UV light (UVP Pen-Ray) for 30 min before use. This vapor lamp produces intense UV irradiation and ozone. The combination of UV irradiation and ozone effectively vaporizes organic debris that accumulates on silicon/nitride surfaces [21]. Scan rates were approximately  $10\text{ mm/s}$  and scan forces were maintained below  $1\text{ nN}$ , which was high enough to achieve good contrast. The force curves (Fig. 1) were obtained under the same conditions, before imaging. These experiments were done

using  $0.1\text{ M}$  phosphate buffer (PBS) and actin buffer, both pH 7.0.

All the images were processed using NIH imaging software, and the force curves were analyzed using Igor 4.03 software (Wavemetrics Inc., Oregon).

### 3. Results and discussion

Although the chemical treatment with nickel does not modify the surface structure of mica [20], force spectroscopy used to measure interaction between the tip and Ni-mica in phosphate and actin buffers revealed a larger dispersion of these interactions in comparison with untreated mica (Fig. 1). Furthermore, the interaction force with Ni-mica was slightly greater than that with untreated mica. According to the model proposed by Souza et al. [22], this reflects differences in dielectric exchange forces that occur when the nickel atoms on the mica surface modify the double-layer properties at the mica surface. Force measurements collected from different points on the mica surface yield a more disperse histogram because of an inhomogeneous nickel distribution.

We also noted that the interaction between the tip and the substrate in phosphate buffer (Fig. 1b) was less than that in actin buffer (Fig. 1a), which may be a result of the higher ionic strength in the phosphate buffer. All of the images shown were obtained using actin buffer.

The first protein images were obtained by depositing F-actin on freshly cleaved, untreated mica without rinsing (Fig. 2). Image acquisition was unsuccessful due to low stability of the deposited sample. During the scans the samples were swept away, and only a few particles remained. Their dimensions ( $2\text{--}6\text{ nm}$ ) were consistent with those of actin monomers ( $3.5\text{--}6\text{ nm}$ ) [23], suggesting that at least part of the F-actin depolymerized when it was diluted from  $10\text{ mg/ml}$  to  $5\text{ }\mu\text{g/ml}$ . Rarely, it was possible to observe some filaments in the first scan (Fig. 3).

Using Ni-mica as substrate, a completely different image was observed (Fig. 4). The samples prepared by depositing actin droplets on Ni-mica produced an irregular network of ridges and val-

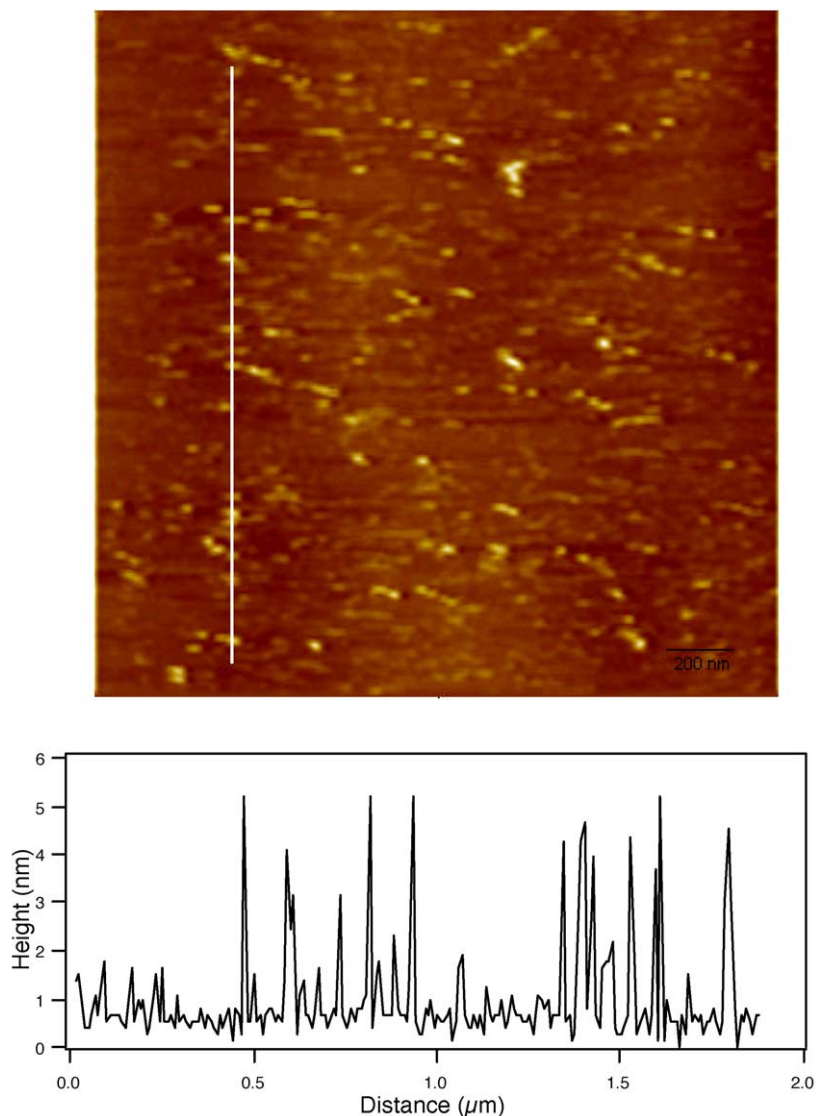


Fig. 2. After deposition of F-actin (5  $\mu\text{g}/\text{ml}$  in actin buffer 6.5 mM KCl) on untreated mica, scanning revealed only scattered particles. The profile along the vertical line shows that such particles have dimensions similar to those of G-actin. Scale bar is 200 nm.

leys. These samples had the appearance of an actin gel rather than F-actin. The association between filaments can increase due to cross-linking and bundling when minute quantities of actin-binding proteins such as filamins are present, so that the whole filament network becomes stiffer [13]. However, since the gel was observed only with

Ni-mica, we infer that  $\text{Ni}^{2+}$  itself favors cross-linking between actin filaments, as described for experiments carried out in solution [24–26].

In order to correlate the effect of  $\text{Ni}^{2+}$  deposited on the mica surface with the extent of actin gel formation, we compared actin images obtained using three different actin concentrations, without

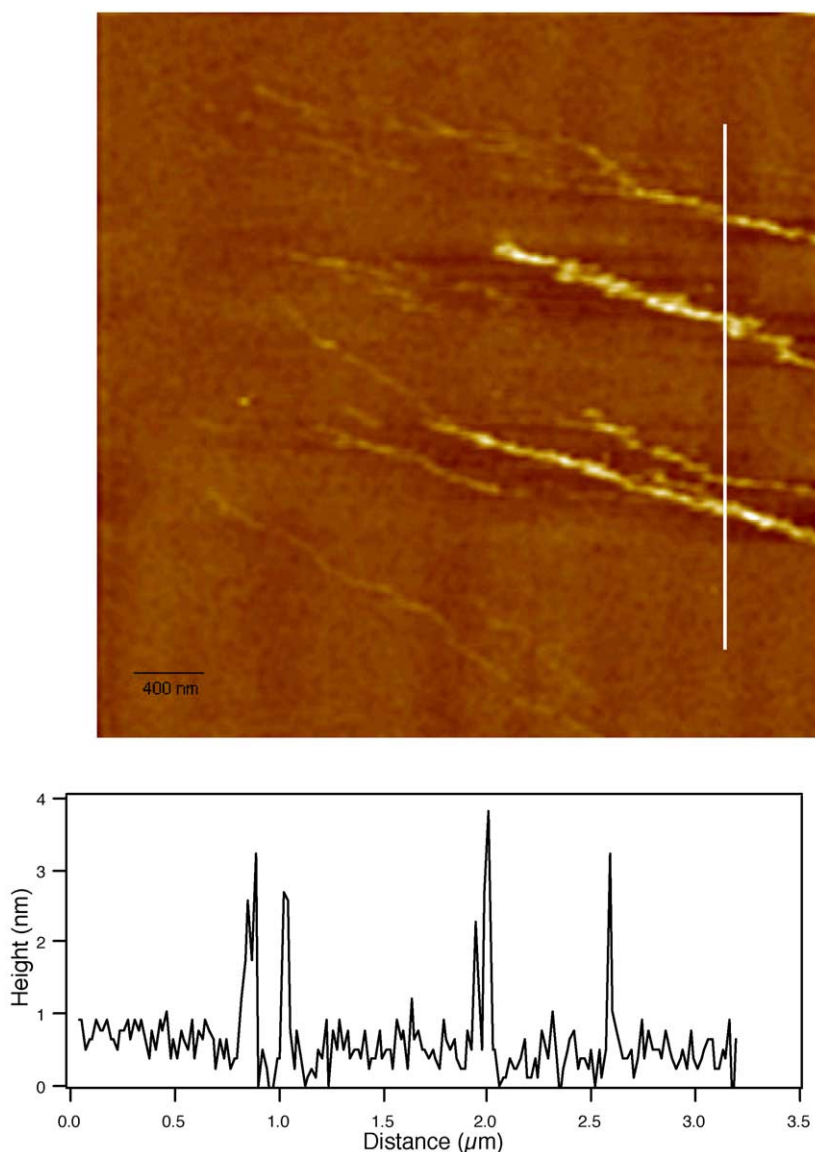


Fig. 3. After deposition of F-actin (5  $\mu\text{g}/\text{ml}$  in actin buffer 150 mM KCl) on untreated mica, scanning revealed few F-actin polymers. Scale bar is 400 nm.

(Fig. 5a–c) and with (Fig. 5d–f) treatment of the mica with 1 mM  $\text{Ni}^{2+}$ .

The images clearly show a progressive increase in density of the actin gel structure as the actin concentration is increased from 3 to 10  $\mu\text{g}/\text{ml}$  on Ni-mica, different from the images of scattered monomers obtained using freshly cleaved mica as

substrate. The surface charge on mica in the absence of counterions is two negative charges per  $\text{nm}^2$  [20,27]. Taking into account the mica film area of  $\sim 1 \text{ cm}^2$  covered by the sample in actin buffer (4  $\mu\text{l}$ ), we can estimate the number of negative charges at approximately  $2 \times 10^{14}$ . Prolonged treatment with an excess of  $\text{Ni}^{2+}$  should

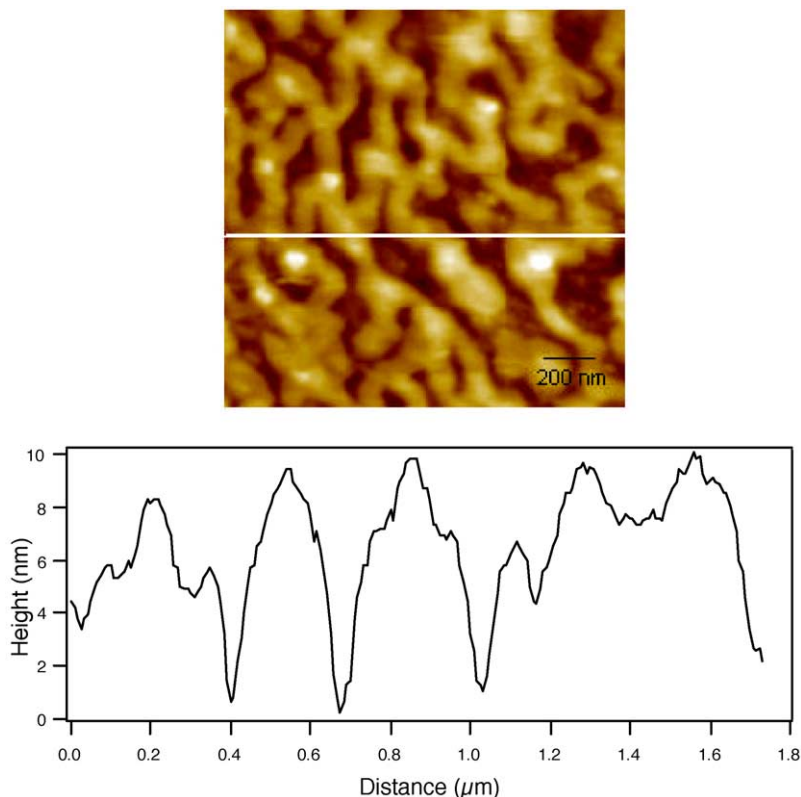


Fig. 4. F-actin (5  $\mu\text{g}/\text{ml}$  in actin buffer 6.5 mM KCl) deposited on Ni-mica. Scale bar is 200 nm.

saturate these sites, and after the sample is deposited onto the mica the  $\text{Ni}^{2+}$  should re-distribute between the surface sites and the sample buffer, where it can bind to the actin and promote gel formation. The upper limit for the concentration of  $\text{Ni}^{2+}$  in the sample droplet is  $2 \times 10^{14}/10^{23} = 2 \times 10^{-9}$  mol in 4  $\mu\text{l}$ , or 0.5 mM. Miki and Wahl [28] have shown that the critical protein concentration for polymerization of actin decreases sharply with this concentration of  $\text{Ni}^{2+}$ , which is more than enough to saturate a class of low-affinity sites on G-actin ( $K_d \sim 60 \mu\text{M}$ ) [25] that promote actin gel formation.

Additional evidence for a greater stability of actin adsorbed to Ni-mica was shown by repeatability from run to run over the same area. The second image was essentially unchanged by the scanning procedure (not shown). These observations indicate that  $\text{Ni}^{2+}$  provides a bridge between

actin and Ni-mica. The importance of  $\text{Ni}^{2+}$  in stabilizing the actin–mica attachment may lie in its ability to form coordination complexes with nitrogen and oxygen atoms; many of these complexes are octahedral or tetragonal [29]. Furthermore, nickel has a high ionization potential, which would favor formation of stable coordination complexes between the negatively charged mica surface and the negatively charged actin.

Although no sample movement was observed during scans on Ni-mica, rinsing the deposited samples with water or buffer removed all of the protein, indicating that the strength of the actin–Ni-mica bond is limited.

#### 4. Conclusions

AFM imaging requires sample immobilization on a flat substrate. Mica is the most suitable



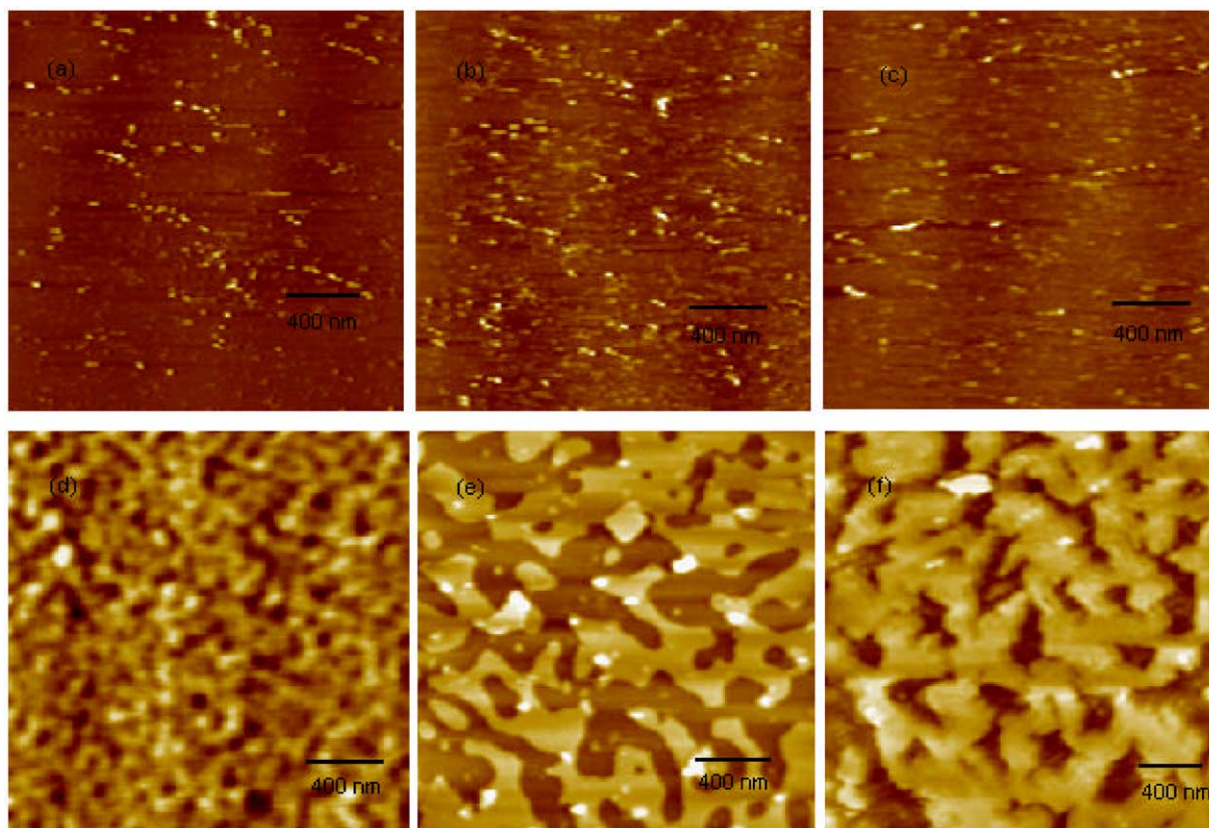


Fig. 5. F-actin (in actin buffer 6.5 mM KCl) deposited on mica (a) 3  $\mu\text{g/ml}$ ; (b) 5  $\mu\text{g/ml}$ ; (c) 10  $\mu\text{g/ml}$ ; and deposited on Ni-mica (d) 3  $\mu\text{g/ml}$ ; (e) 5  $\mu\text{g/ml}$ ; (f) 10  $\mu\text{g/ml}$ . All scale bars are 400 nm.

substrate for obtaining AFM images with molecular resolution. Nevertheless, visualization of negatively charged samples on mica requires specific approaches to stabilize them by modifying either the sample environment or the mica surface to increase sample stability during the tip scan.

In this report we have adapted a method of preparing Ni-mica that appears to increase the affinity of mica for actin. However, actin filaments appear on Ni-mica as an actin gel, possibly due to a tendency for  $\text{Ni}^{2+}$  to promote polymerization of G-actin and side-to-side aggregation of F-actin filaments.

Additionally, force spectroscopy suggests that this treatment promotes a modification in the double-layer properties of mica film, resulting in an increase in interaction between tip and Ni-mica.

## Acknowledgments

Financial support was provided by Brazilian agencies FAPERGS, CAPES, FUJB, PADCT and CNPq. We thank Débora M. Araujo for preparing the actin.

## References

- [1] G. Binnig, C.F. Quate, C. Gerber, Atomic force microscope, *Phys. Rev. Lett.* 56 (1986) 930–933.
- [2] E.L. Florin, V.T. Moy, H.E. Gaub, Adhesion forces between individual ligand–receptor pairs, *Science* 264 (1994) 415–417.
- [3] D.A. Walters, J.P. Cleveland, N.H. Thomson, et al., Short cantilevers for atomic force microscopy, *Rev. Sci. Instrum.* 67 (1996) 3583–3590.
- [4] P.K. Hansma, V.B. Elings, O. Marti, S.A. Gould, C.E. Bracker, Scanning tunneling microscopy and atomic force microscopy: application to biology and technology, *Science* 242 (1988) 209–216.
- [5] T. Thundat, D.P. Allison, R.J. Warmack, et al., Atomic force microscopy of DNA on mica and chemically modified mica, *Scanning Microsc.* 6 (1992) 911–918.
- [6] J. Vesenka, M. Guthold, C.L. Tang, D. Keller, E. Delaine, C. Bustamante, Substrate preparation for reliable imaging of DNA molecules with the scanning force microscope, *Ultramicroscopy* 42 (1992) 1243–1249.
- [7] M. Bezanilla, B. Drake, E. Nudler, M. Kashlev, P.K. Hansma, H.G. Hansma, Motion and enzymatic degradation of DNA in the atomic force microscope, *Biophys. J.* 67 (1994) 2454–2459.
- [8] H.G. Hansma, D.E. Laney, M. Bezanilla, R.L. Sinsheimer, P.K. Hansma, Applications for atomic force microscopy of DNA, *Biophys. J.* 68 (1995) 1672–1677.
- [9] C.R. Ill, V.M. Keivens, J.E. Hale, et al., A COOH-terminal peptide confers regiospecific orientation and facilitates atomic force microscopy of an IgG1, *Biophys. J.* 64 (1993) 919–924.
- [10] T.D. Pollard, J.A. Cooper, Actin and actin-binding proteins. A critical evaluation of mechanisms and functions, *Ann. Rev. Biochem.* 55 (1986) 987–1035.
- [11] T.D. Pollard, Actin, *Curr. Opin. Cell Biol.* 2 (1990) 33–40.
- [12] K.C. Holmes, D. Popp, W. Gebhard, W. Kabsch, Atomic model of the actin filament, *Nature* 347 (1990) 44–49.
- [13] J.H. Hartwig, T.P.J. Stossel, Structure of macrophage actin-binding protein molecules in solution and interacting with actin filaments, *J. Mol. Biol.* 145 (1981) 563–581.
- [14] T.D. Pollard, U. Aebi, J.A. Cooper, W.E. Fowler, P. Tseng, Actin structure, polymerization, and gelation, *Cold Spring Harb. Sym. Quant. Biol.* 46 (1982) 513–524.
- [15] Z. Shao, D. Shi, A.V. Somlyo, Cryoatomic force microscopy of filamentous actin, *Biophys. J.* 78 (2000) 950–958.
- [16] D. Shi, A.V. Somlyo, A.P. Somlyo, Z. Shao, Visualizing filamentous actin on lipid bilayers by atomic force microscopy in solution, *J. Microsc.* 201 (2001) 377–382.
- [17] M. Fritz, M. Radmacher, J.P. Cleveland, et al., Imaging globular and filamentous proteins in physiological buffer solutions with tapping mode atomic force microscopy, *Langmuir* 11 (1995) 3529–3535.
- [18] J.D. Pardee, J.A. Spudich, Purification of muscle actin, *Methods Enzymol.* 85 (1982) 164–181.
- [19] A.G. Gornall, C.J. Bardawill, M.M. David, Determination of serum proteins by means of the biuret reaction, *J. Biol. Chem.* 177 (1949) 751–766.
- [20] H.G. Hansma, D. Laney, DNA binding to mica correlates with cationic radius: assay by atomic force microscopy, *Biophys. J.* 70 (1996) 1933–1939.
- [21] W. Kern, *Handbook of Semiconductor Wafer Cleaning Technology*, Noyes Publications, Park Ridge, NJ, 1993.
- [22] E.F. Souza, G. Ceotto, O.J. Teschke, Dielectric constant measurements of interfacial aqueous solutions using atomic force microscopy, *J. Mol. Catal. A: Chem.* 167 (2001) 235–243.
- [23] P. Shterline, J. Clayton, J. Sparrow, Actin, *Protein Profile* 2 (1995) 1–103.
- [24] H. Strzelecka-Golaszewska, E. Pröchniewicz, W. Drabikowski, Interaction of actin with divalent cations. 1. The effect of various cations on the physical state of actin, *Eur. J. Biochem.* 88 (1978) 219–227.
- [25] H. Strzelecka-Golaszewska, E. Pröchniewicz, W. Drabikowski, Interaction of actin with divalent cations. 2. Characterization of protein-metal complexes, *Eur. J. Biochem.* 88 (1978) 229–237.
- [26] I. DalleDonne, A. Milzani, C. Ciapparelli, M. Comazzi, M.R. Gioria, R. Colombo, The assembly of  $\text{Ni}^{2+}$ -actin: some peculiarities, *Biochim. Biophys. Acta* 1426 (1999) 32–42.



- [27] R.M. Pashley, J.N. Israelachvili, DLVO and hydration forces between mica surfaces in  $\text{Mg}^{2+}$ ,  $\text{Ca}^{2+}$ ,  $\text{Sr}^{2+}$ , and  $\text{Ba}^{2+}$  chloride solutions, *J. Colloid. Interf. Sci.* 97 (1984) 446–455.
- [28] M. Miki, P. Wahl, Fluorescence energy transfer between points in G-actin: the nucleotide-binding site, the metal-binding site and Cys-373 residue, *Biochim. Biophys. Acta* 828 (1985) 188–195.
- [29] E.T. Snow, L. Xu, P.L. Kinney, Effects of nickel ions on polymerase activity and fidelity during DNA replication in vitro, *Chem. Biol. Interact.* 88 (1993) 155–173.